Supporting Information for

Encapsulation of OZ439 into Nanoparticles for Supersaturated Drug Release in Oral Malaria Therapy

Hoang D. Lu[1±], Kurt D. Ristroph[1±], Ellen L. K. Dobrijevic[1±], Jie Feng[1], Simon A. McManus[1], Yingyue Zhang[1], William D. Mulhearn[1], Hanu Ramachandruni[2], Anil Patel[2], Robert K. Prud'homme[1]*

[1]*Department of Chemical and Biological Engineering, A301 Engineering Quadrangle, Olden St., Princeton University, Princeton, New Jersey 08854, United States*

[2]*Medicines for Malaria Venture, Route de Pré-Bois 20, 1215 Meyrin, Switzerland*

±: co-first author

*to whom correspondence should be addressed; E-mail: prudhomm@princeton.edu

Supplementary Figures

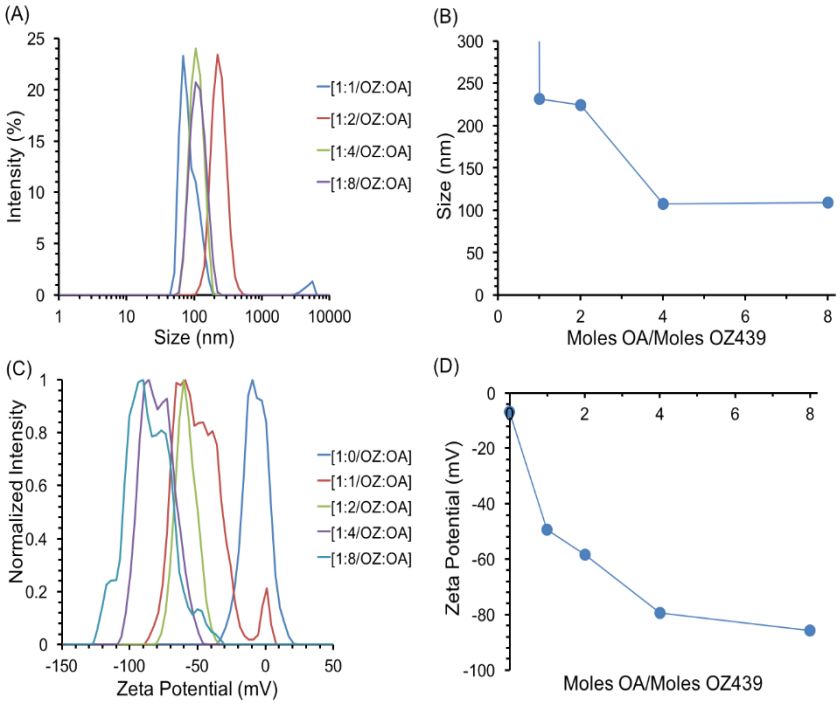

Figure S1: Characteristic DLS properties over time of OZ439 nanoparticles with varying molar ratios of OA and no stabilizer; size distribution at t=0 hours (A), average size as a function of molar ratio of OA to OZ439 (B), zeta potential distribution (C) and average zeta potential as a function of molar ratio of OA to OZ439 (D). (A) demonstrates that ratios of OZ439 to OA of 1:2, 1:4 and 1:8 initially formed nanoparticles, while 1:1 produced nanoparticles with some aggregates. OZ439 nanoparticles without OA immediately formed aggregates and are therefore not included (A). The size of the nanoparticles decreased with increasing OA; this could be the result of increased nucleation (B). All nanoparticle formulations had a negative surface charge (C). Increasing the molar ratio of OA led to more negative surface charges (D).

The most stable of these stabilizer-free formulations was at a ratio of 1:4 OZ439:OA. These nanoparticles did not show significant changes in size and maintained a narrow size distribution with only a small amount of precipitate evident at 28 hours (Figure S2-A S2-B). Although these NPs were stable enough to allow for further processing, zeta potential measurements showed that they possessed a highly-charged surface (Figure S1-C). Particles with charged surfaces are prone to flocculation in environments with varying pH and high salt

concentrations, such as the GI tract; furthermore, high surface charge increases protein binding, which leads to faster clearance *in vivo*[12]. Thus such charge-stabilized NPs are less desirable than sterically-stabilized particles, which do not display such high stability dependence on pH and salt concentration.

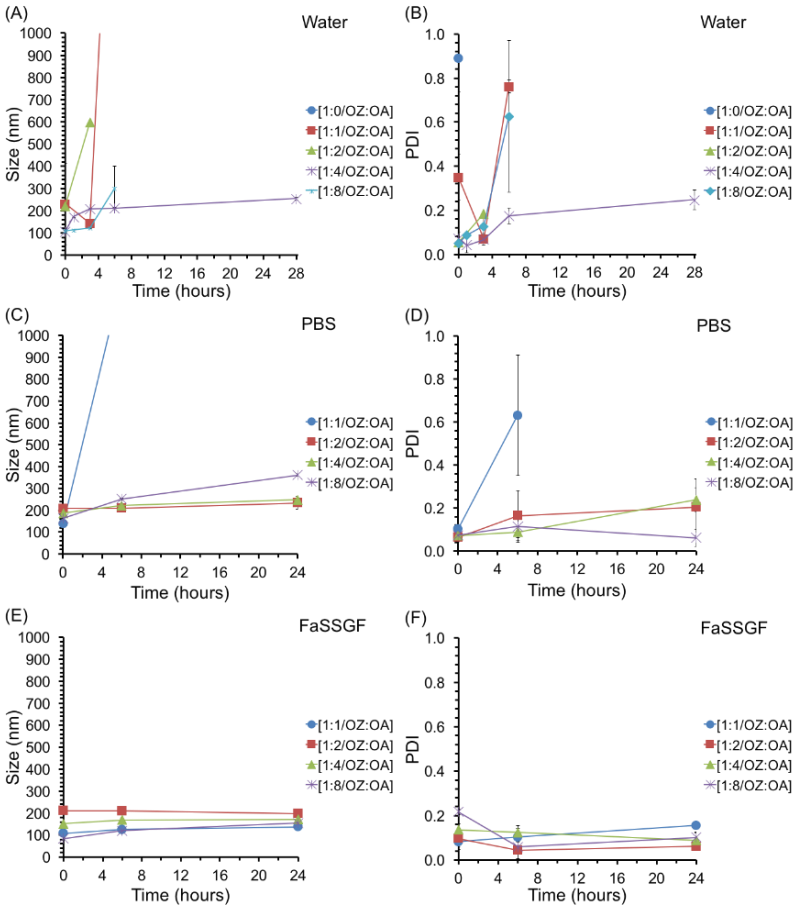

Figure S2: The average size and PDI over time of nanoparticles with varying molar ratios of OZ439 to OA in water (A&B), PBS (C&D) and FaSSGF (E&F). A ratio of OZ439 to OA of 1:4 was the most stable in water over 28 hours. A molar ratio of OZ439 to OA of 1:0 formed large aggregates immediately, while 1:2 was stable for 3 hours and 1:1 and 1:8 were stable for 6 hours. The high concentration of ions in PBS shielded the negative surface charge of the nanoparticles with 1:1 OZ439 to OA, leading to faster aggregation in PBS than water (C). The lower concentration of ions in gastric fluid did not lead to charge shielding and aggregation (E&F). The stability in gastric fluid could be the result of the lower solubility of OZ439 in FaSSGF of 9.8μg/mL compared to 4.25mg/mL in water.

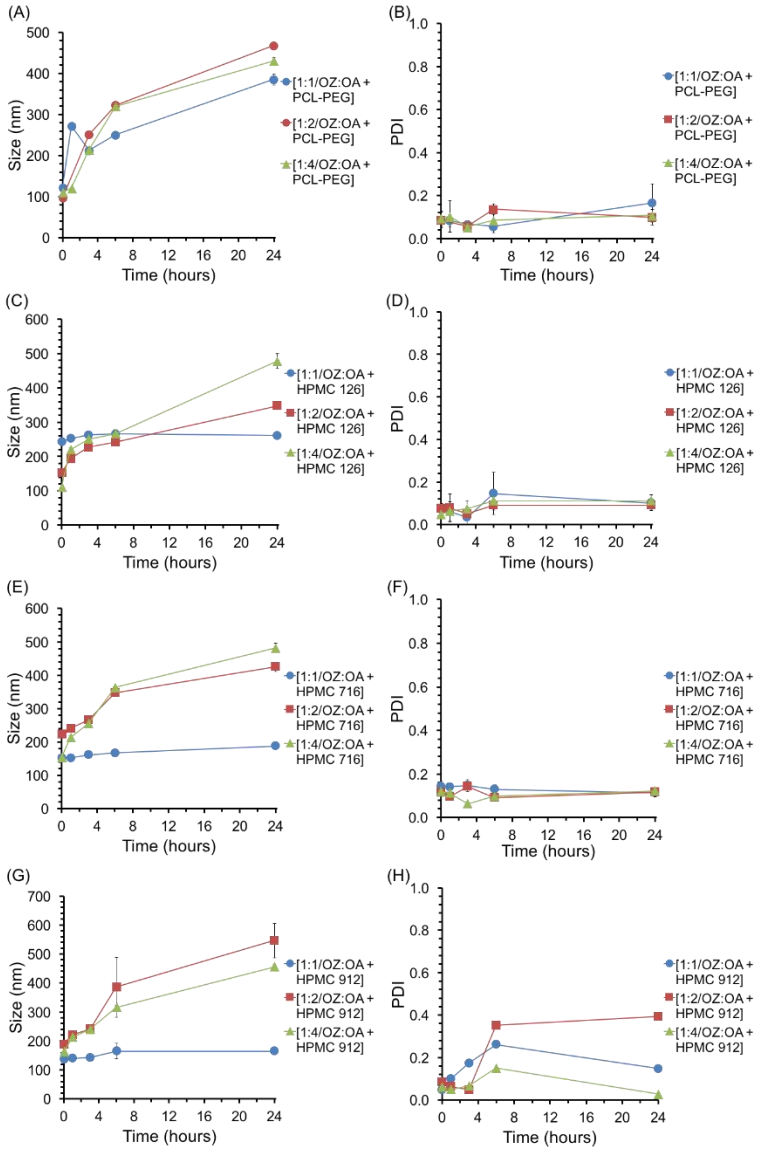

Figure S3: Nanoparticles with ratios of OZ439:OA of 1:1, 1:2 and 1:4 with stabilizers PCL-PEG (A&B), HPMC 126 (C&D), HPMC 716 (E&F) and HPMC 912 (G&H). The average size and PDI over time are shown to compare stability of formulations. PCL-PEG stabilized nanoparticles increased in size significantly over time (A). For each HPMC stabilizer 1:1 OZ439 to OA was the most stable, all remained within 25% of their initial average size. Nanoparticles with HPMC 126 or 716 maintained a narrow size distribution, with their PDI remaining under 0.2 over 24 hours (D&F). However, for HPMC 912 the PDI reached a maximum of 0.26±0.07, 0.39±0.21 and 0.15±0.04 for 1:1, 1:2 and 1:4 OZ439 to OA respectively. The most promising formulations were 1:1 OZ439:OA with either HPMC 126 or HPMC 716 as a stabilizer, increasing in average size by only 9% and 24% respectively (C&E).

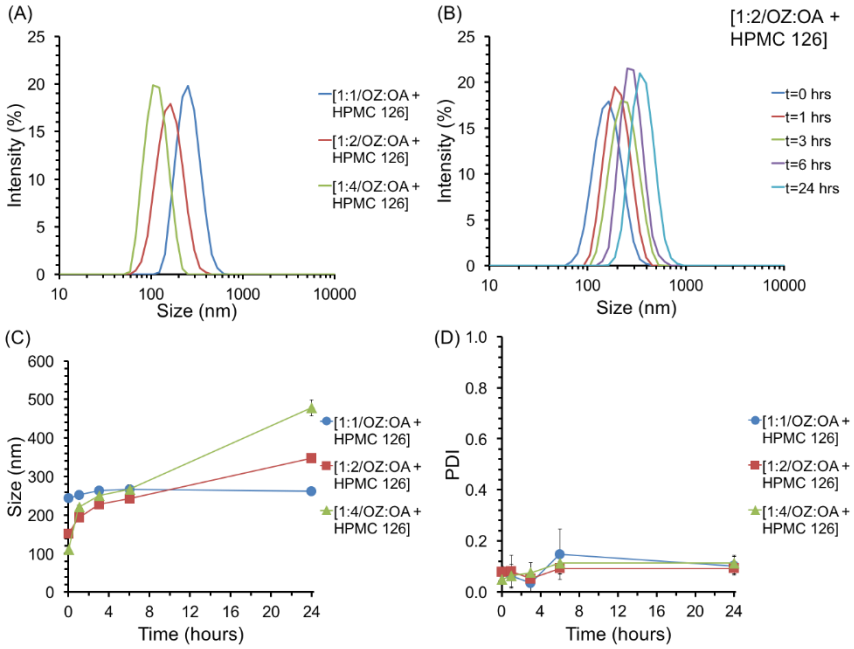

Figure S4: Nanoparticle formulations with molar ratios of OZ439:OA of 1:1, 1:2 and 1:4 with the polymer HPMC 126, comparison of initial size distribution (A), average size (C) and PDI (D) over time for 24 hours. Increasing the molar ratio of OZ439 to OA decreased the size of the nanoparticles, this could be a result of increased nucleation (A). The average size of the nanoparticles increased by 23 ± 18nm, 90 ± 7nm and 156 ± 5nm over 6 hours for OZ439:OA ratios of 1:1, 1:2 and 1:4 respectively (C). Although all nanoparticle formulations tested swelled over time, the PDI of all remained under 0.2, indicating a narrow size distribution was maintained (D). The molar ratio of OZ439:OA of 1:1 with HPMC 126 produced the most stable nanoparticles. The size distribution over time of 1:2 OZ439 to OA nanoparticles showed that although the size increased over 24 hours from an average size of 152 ± 3nm to 348 ± 2nm no aggregates above 1000nm appeared (B).

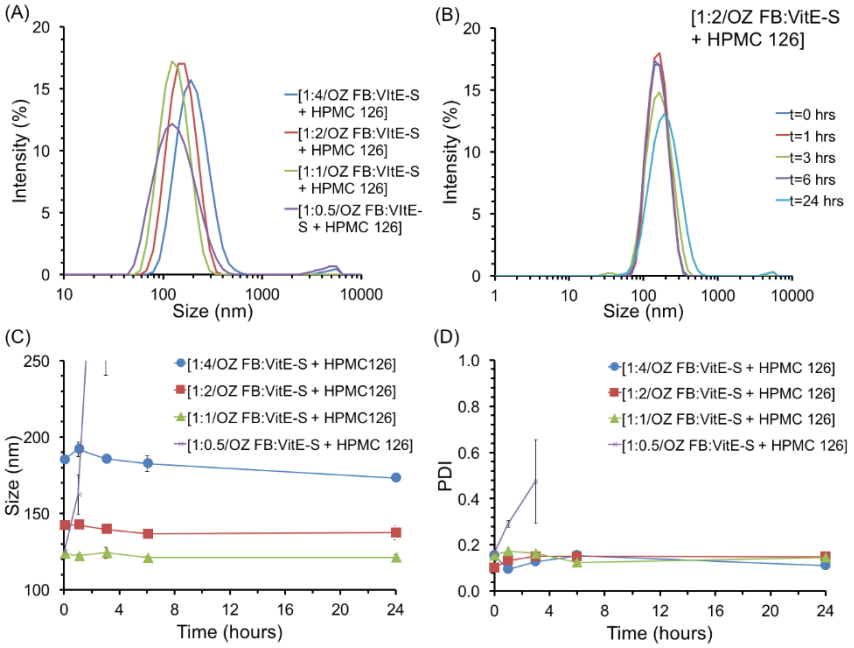

Figure S5: Effect on nanoparticle stability of changing the ratio of OZ FB to VitE-S, with HPMC 126. The initial size distribution of each formulation tested, with ratios of OZ FB to VitE-S of 1:0.5, 1:1, 1:2 and 1:4 demonstrate that increasing concentrations of VitE-S led to larger nanoparticles (A). The size distribution over time for nanoparticles with 1:2 OZ FB to VitE-S and HPMC 126 shows the stability of the nanoparticles, at 24 hours there was a small fraction of nanoparticles greater than 1000nm (B). The average size over time, demonstrates the increase in size with increasing concentrations of VitE-S, as well as the stability of nanoparticles with OZ FB to VitE-S ratios of 1:1, 1:2 and 1:4 (C). Nanoparticles with a ratio of 1:0.5 swelled in size over 3 hours and reached a PDI of 0.47 ± 0.18, while the PDI of the other formulations all remained below 0.2 over 24 hours (D). Together these figures demonstrate that OZ FB to VitE-S ratios of 1:1, 1:2 and 1:4 produced stable nanoparticles, while a ratio of 1:0.5 did not produce stable nanoparticles.

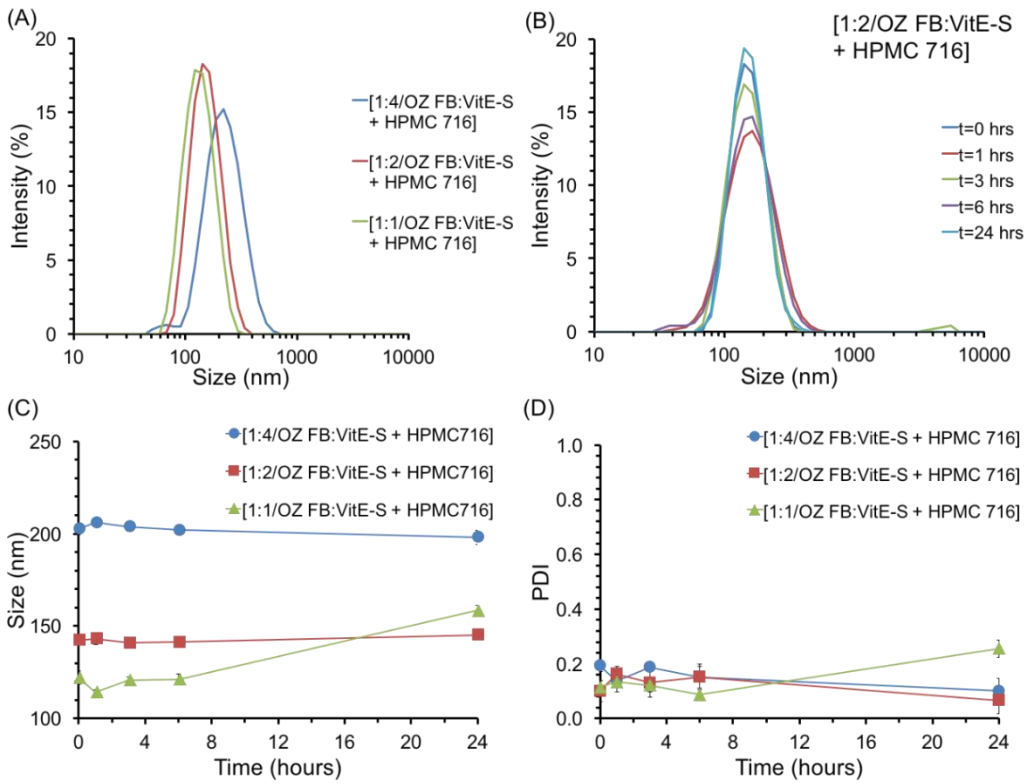

Figure S6: OZ FB nanoparticles with HPMC 716 and varying molar ratios of OZ FB to VitE-S. The initial size distribution of each formulation tested, with ratios of OZ FB to VitE-S of 1:1, 1:2 and 1:4 demonstrates that increasing concentrations of VitE-S led to larger nanoparticles (A). The size distribution over time for nanoparticles with 1:2 OZ FB to VitE-S and HPMC 126 shows the stability of the nanoparticles; at 3 hours, there was a small fraction of nanoparticles greater than 1000nm (B). The average size over time, demonstrates the increase in size with increasing concentrations of VitE-S, as well as the stability of nanoparticles with OZ FB to VitE-S ratios of 1:2 and 1:4 (C). Nanoparticles with OZ FB to VitE-S ratio of 1:1 were stable for the first 6 hours, but there was a moderate increase in size at 24 hours and increase in PDI (C&D).

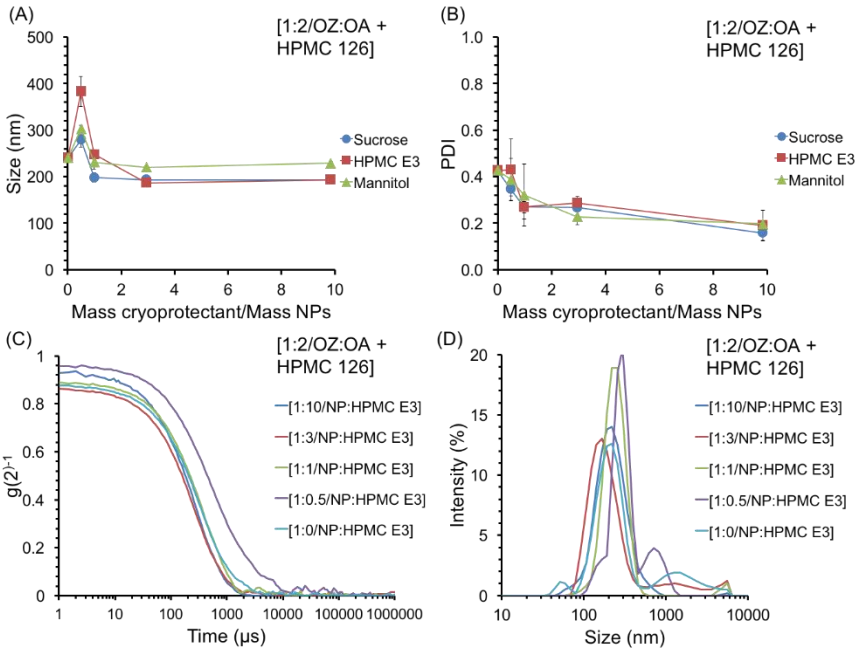

Figure S7: The effect of species and amount of cryoprotectant on average size (A) and PDI (B) of re-dispersed lyophilized powder of 1:2 OZ439 to OA nanoparticles with the stabilizer HPMC 126. HPMC E3 was the most promising cryoprotectant, the correlogram (C) and size distribution (D) of the re-dispersed powders with varying mass ratios of nanoparticle to HPMC E3 are shown. For nanoparticles:cryoprotectant mass ratios above 1:1 the average size of the re-dispersed nanoparticles was relatively constant, at 195± 2nm, 209± 28nm and 227± 5nm for sucrose, HPMC E3 and mannitol respectively (A). The PDI decreased with increasing amounts of cryoprotectant, indicating that higher levels of cryoprotectant protected nanoparticles against aggregation or instability in the lyophilization process (B). The correlogram demonstrates that for all levels of HPMC E3 cryoprotectant added the re-dispersed suspension primarily contained nanoparticles of a tight size distribution (C). Increasing the amount of HPMC E3 cryoprotectant generally reduced the level of aggregates present on re-dispersion, there was only a small tail of aggregates present in the size distribution at 1:1, 1:3 and 1:10 mass of nanoparticles to HPMC E3 (D).

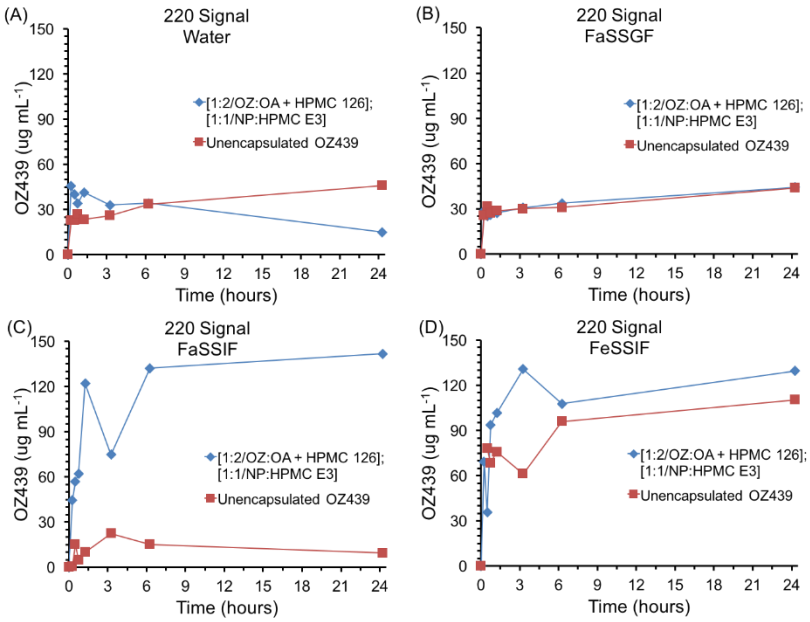

Figure S8: Release rates of lyophilized nanoparticles and unencapsulated OZ439. The powders were added to a total concentration of 140µg/mL and incubated in either water (A), FaSSGF (B), FaSSIF (C) or FeSSIF (D). The concentration of free OZ439 was measured in the solution over 24 hours to indicate the release of OZ439 in different bio-media. In water and FaSSGF the maximum concentration achieved by both nanoparticles and unencapsulated powder was 45µg/mL (A&B). The maximum concentration of OZ439 released from nanoparticles was 142 and 131µg/mL in FaSSIF and FeSSIF respectively (C&D). In FaSSIF, the concentration of OZ439 in solution was on average 9 times higher from nanoparticles than unencapsulated powder and all OZ439 was released from the nanoparticles (C). The concentration after 24 hours approached 140µg/mL for both the nanoparticles and unencapsulated powder in FeSSIF (D).

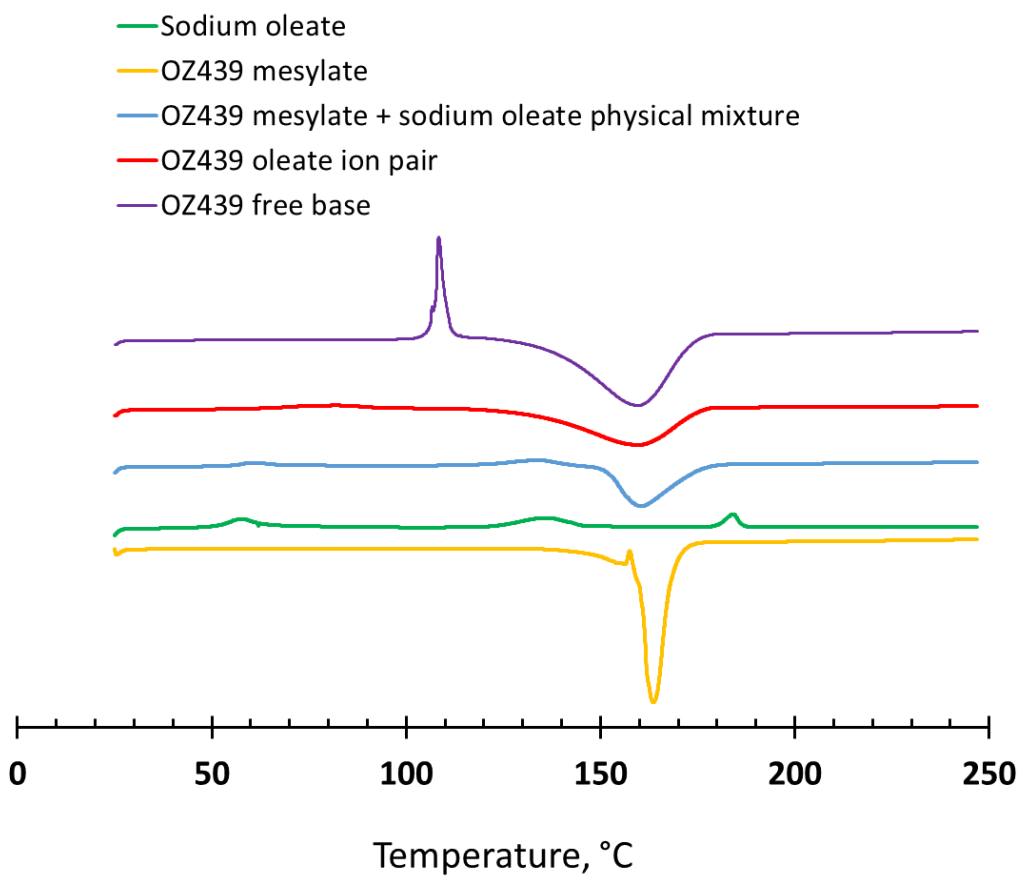

Figure S9: Differential scanning calorimetry profiles for sodium oleate (green), OZ439 mesylate (yellow), a physical mixture of sodium oleate and OZ439 mesylate with masses corresponding to the 1:2 molar ratio used in the text (blue), isolated OZ439 oleate hydrophobic ion paired complex (red), and OZ439 free base (purple). The physical mixture contains elements of the individual component curves that are not present in the ion paired complex; for example, the slight peaks at 60°C and 140°C. The ion paired complex's profile contains a peak note present in any of the other profiles (80°C). The differences among the profiles suggest the formation of a hydrophobic ion paired complex between OZ439 cation and oleate anion.

DSC measurements were performed using a TA Instruments Q200 (New Castle, DE). 5-10 mg of sample was weighed into an aluminum pan and equilibrated at 20 °C under nitrogen (50 mL/min). Subsequently, the samples were heated from 20 to 250 °C at a heating rate of 5 °C/min. The scan was analyzed by TA Instruments Universal Analysis 2000 software.